Electronic Supplementary Material (ESI) for Nanoscale.
This journal is © The Royal Society of Chemistry 2020

# 2D-based Floating Gate Device with Linear Synaptic Weight Update

*Eunpyo Park[1,3], Minkyung Kim[1,4], Tae Soo Kim[6], In Soo Kim[2], Jongkil Park[1], Jaewook Kim[1], YeonJoo Jeong[1], Suyoun Lee[1], Inho Kim[1], Jong-Keuk Park[1], Gyu Tae Kim[3], Jiwon Chang[5,]*, Kibum Kang[6,]*, Joon Young Kwak[1,]**

[1]Center for Neuromorphic Engineering, Korea Institute of Science and Technology (KIST), Seoul, 02792, South Korea

[2]Nanophotonics Research Center, Korea Institute of Science and Technology (KIST), Seoul, 02792, South Korea

[3]School of Electrical Engineering, Korea University, Seoul, 02841, South Korea

[4]Department of Materials Science and Engineering, Korea University, Seoul, 02841, South Korea

[5]Department of Electrical and Computer Engineering, Ulsan National Institute of Science and Technology (UNIST), Ulsan 44919, South Korea

[6]Department of Materials Science and Engineering, Korea Advanced Institute of Science and Technology (KAIST), Daejeon 34141, South Korea

## Supporting Information

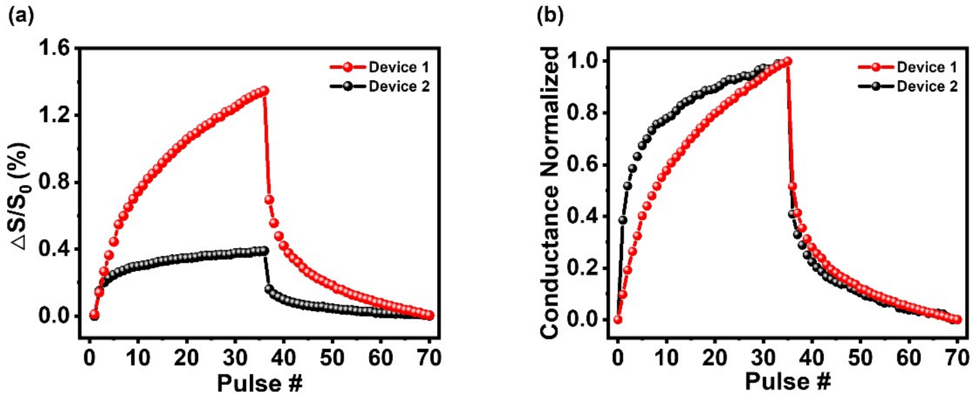


**Figure S1.** Effects of coupling ratio on synaptic weight updates

To demonstrate the effects of coupling ratio on non-linearity factor of synaptic weight update, we additionally fabricated two types of devices with different gate stacks. They have the same MOCVD-grown $MoS_2$ channel, 14nm of $Al_2O_3$ tunnel oxide, and CVD-grown graphene floating gate, except different blocking oxides, which determine the coupling ratio of the devices. Device 1 has the blocking oxide of 24 nm $HfO_2$ (k ~ 25), while Device 2 has 28 nm of $Al_2O_3$ (k ~ 10). The calculated coupling ratios of the fabricated devices are approximately 0.59 for Device 1 and 0.33 for Device 2. The same voltage pulse trains were applied on both devices; –15 V with 0.1 msec pulse width for potentiation and +13 V with 0.1 msec pulse width for depression. The device with the higher coupling ratio (Device 1) shows the higher On/Off ratio (Figure S2a) and the better non-linearity (Figure S2b) as expected.

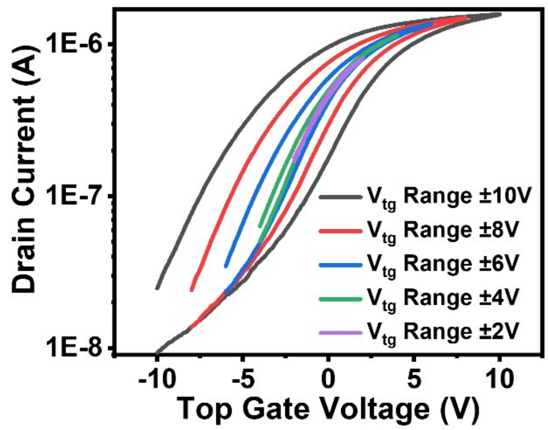


**Figure S2.** Transfer curves with various $V_{tg}$ sweep

Figure S2 shows the transfer curves ($I_{ds} - V_{tg}$) measured at various sweeping ranges of $V_{tg}$. For the proper memory characteristics, applying voltage over 4 V amplitude is needed as the memory windows are open from $V_{tg}$ range over ±4 V. Based on the results, we optimized the voltage pulse conditions for potentiation and depression measurements.

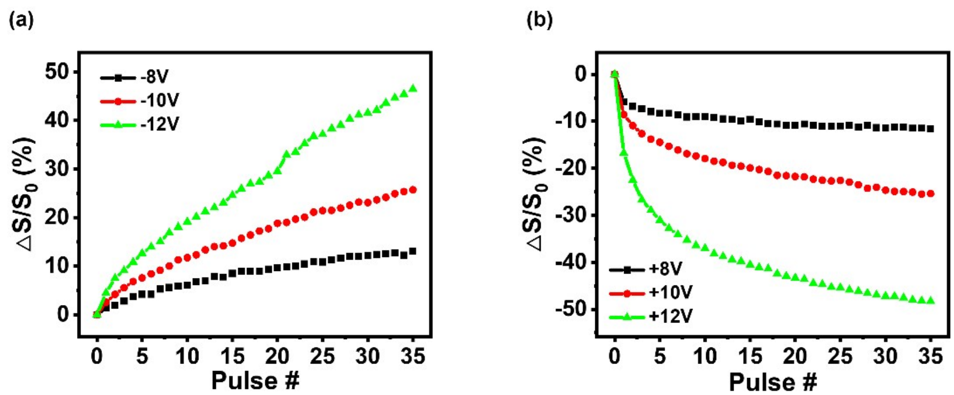


**Figure S3.** Synaptic weight updates in potentiation and depression with different voltage pulse amplitudes

Figure S3 shows synaptic weight updates with different pulse amplitudes for potentiation and depression operations. For each curve, different voltage pulse amplitude with 1 μs pulse width is applied for thirty-five times, consecutively.

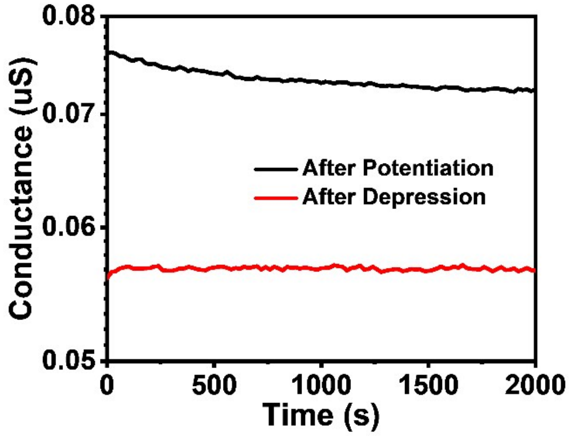


**Figure S4.** Synaptic weight data retention times

Retention characteristics in two different conductance states are measured at room temperature. For the experiments, thirty-five times of −10 V voltage pulses with 10 μs pulse width are applied to set a conductance level at time zero for a potentiation case and thirty-five times of +8 V voltage pulses with 10 μs pulse width are applied to set a conductance level at time zero for a depression case. We read the conductance level every 1 second for 2,000 seconds. 5% of conductance change after potentiation and 2% conductance change after depression are observed.